JOURNAL OF SOLID STATE CHEMISTRY 77, 180–189 (1988)

Lithium Insertion into Fe_3O_4

M. S. ISLAM*

Department of Chemistry, University College London, 20 Gordon St., London WC1H 0AJ, United Kingdom

AND C. R. A. CATLOW

Department of Chemistry, University of Keele, Keele, Staffs ST5 5BG, United Kingdom

Received February 25, 1988

Theoretical techniques are used to examine the effect of lithium insertion into the spinel Fe_3O_4. Particular attention is focused on the sites occupied by the intercalating cation and the extent of aggregation. Our results support the models in which insertion proceeds with reduction and displacement of the tetrahedrally coordinated Fe^{3+} to produce the ordered rock-salt structured phase, $LiFe_3O_4$. In addition the defect and transport properties of the rock-salt phase are investigated. The calculations suggest that lithium Frenkel disorder will dominate and that lithium ion migration is via an interstitialcy mechanism. © 1988 Academic Press, Inc.

1. Introduction

Transition metal oxides, into which mobile ions may be reversibly inserted (or extracted) to give a wide range of solid solutions, are of interest for possible application as electrodes in batteries and electrochromic displays. These reactions also permit the synthesis of compounds at low temperature that may be inaccessible by any high-temperature method. The incentive to find electrode materials has, thus, led to the study of solid-solution systems with tunnel or framework structures as hosts for lithium insertion at ambient temperature. Particular attention has been focused on spinel oxides owing to their close-packed framework structures.

This paper reports the first theoretical study, using simulation techniques, on a relatively simple intercalation problem, i.e., lithium insertion into the spinel, Fe_3O_4. Our study pays careful attention to the sites occupied by the intercalating cation and the extent of aggregation. As a background to the theoretical work, we first discuss previous experimental investigations. Diffraction studies have shown that during the lithiation process Fe^{3+} ions, normally on the tetrahedral sites, are reduced and displaced by the Li^+ ions on to adjacent unoccupied octahedral sites, producing an ordered rock-salt structured phase: $LiFe_3O_4$ (*1*). Therefore, the structural modelling of $LiFe_3O_4$ and the relationship with Fe_3O_4 will also be considered. We conclude the

* Present address: Eastman Kodak Research Laboratories, Rochester, NY 14650-2021, USA.

0022-4596/88 $3.00

study with an investigation of the defect and transport properties of the rock-salt phase, in particular the energetics of lithium ion diffusion.

2. Experimental Studies

An insertion reaction requires reduction of the host matrix and mobility of the intercalate within the host (*2*). High ionic mobility requires structures that contain an interconnected interstitial space with a relatively smooth potential energy surface. Such an interstitial space may consist of isolated one-dimensional (1D) tunnels, isolated 2D layers, or a 3D network within a framework structure (*3*). Since 1D tunnels can be blocked by stacking faults, attention has been focused on 2D and 3D ionic conductors.

2.1 Layered Compounds

The most widely studied solid-solution electrodes for lithium ion insertion have been layered compounds, which permit only 2D lithium ion diffusion (*4–7*). Essentially the insertion process involves the transfer of electrons to the transition metal array from the intercalate (chemical insertion) or from an external electrical circuit (electrochemical insertion).

In the system Li_xTiS_2, for example, the inserted Li^+ ions enter into alternate octahedral site layers of a close-packed hexagonal anion array; charge-neutrality is achieved by introducing electrons into the 3d bands of the TiS_2 layers (*4*). The Li^+ ion mobility is enhanced by the ability of the structure to expand along the *c*-direction. These layered transition metal dichalcogenides MX_2 consist of close-packed layers of MX_6 octahedra, which are stacked on top of each other to form a close-packed anion array. Strong bonding exists within the layers, whereas only van der Waals forces hold the layers together. In these materials the anion layers are prized apart by the Li^+ ions during lithiation. A similar *c*-axis flexibility and Li^+ ion transport are found in the layered oxide $Li_{1-y}CoO_2$ which contains Li^+ ions on alternate octahedral site layers of a cubic close-packed anion array (*5*).

2.2 Framework Structures

The studies on layered compounds demonstrate the stability of Li^+ ions on both octahedral and tetrahedral sites. They also show that Li^+ ions are mobile in a close-packed anion array which has an interconnected space of edge-sharing octahedra. It is therefore of interest to examine the transport properties of lithium in the framework spinel structure and to compare the mobilities in such a 3D structure with those found in the layered compounds.

In general, the $A[B_2]O_4$ spinel structure (space group $Fd3m$) has the *B* cations occupying half of the octahedral sites (the 16d positions) and the *A* cations occupying an eighth of the tetrahedral (8a) sites within a close-packed array of anions (at positions 32e). The unoccupied octahedral (16c) sites form an interconnected 3D array of edge-shared sites, identical to the 16d array, but shifted by half a lattice parameter in space. Each 16c site also shares common faces with two 8a sites which allows a possible migration pathway for the *A* cations.

2.3 Insertion Studies on Fe_3O_4

The possibility that Li^+ ion mobilities in spinel oxides could be adequate for battery applications has led to the investigation of lithium insertion into magnetite. Fe_3O_4 adopts the inverse spinel structure in which the tetrahedral (8a) sites are occupied by Fe^{3+} ions and the remaining iron atoms occupy the octahedral (16d) sites; i.e., it has the following cation valence distribution:

$$Fe^{3+}[Fe^{2+}Fe^{3+}]O_4.$$

From an X-ray diffraction study, Thack-

eray *et al.* (*1*) concluded that, on insertion, the lithium ions occupy the vacant octahedral (16c) sites; repulsive electrostatic forces between the Li^+ ions and the Fe^{3+} ions in neighboring 8a positions displace the Fe^{3+} ions into adjacent 16c sites. This produces the end composition corresponding to the rock-salt-like structured $LiFe_3O_4$, with an expansion of the cubic unit cell. The diffraction analysis shows that the $[Fe_2]O_4$ sublattice, which provides a 3D interstitial space for Li^+ ion transport, remains intact during lithiation. The long-range order of the Fe ions on the octahedral sites is, therefore, not affected by the insertion reaction. Generally, lithiation in excess of $x = 1$ in $Li_xA[B_2]O_4$ causes a breakdown of the structure into products that are difficult to identify (*8*).

From electrochemical information and diffraction data Thackeray *et al.* (*1*) proposed that lithium insertion into Fe_3O_4 follows the pathway:

$$Fe^{3+}_{8a}[Fe^{2+}Fe^{3+}]_{16d}O_4 \xrightarrow[x_c\text{Li}]{}$$

$$Li^+_{x_c}Fe^{2+}_{8a}[Fe^{2+}Fe^{3+}]_{16d}O_4 \xrightarrow[(1-x_c)\text{Li}]{}$$

$$\{Li^+_{1.0}Fe^{2+}\}_{16c}[Fe^{2+}Fe^{3+}]_{16d}O_4,$$

producing the rock-salt phase after the addition of one lithium per formula unit. At a critical concentration, x_c, which is found to have a small value (<0.1), the 8a-Fe^{3+} ions are cooperatively displaced to the 16c sites.

The tetragonal spinel Mn_3O_4 has also been studied to demonstrate how the distortion, due to the presence of Mn^{3+} in excess of a critical concentration (*9*), disappears upon lithiation and reduction of Mn^{3+} to Mn^{2+} (*10–12*). The construction of a satisfactory potential model for the $Li_{1+x}Mn_2O_4$ systems has proved extremely difficult, as lithiation is accompanied by a reduction of Mn^{4+} to Mn^{3+}. The problems arise from the increase in concentration of Mn^{3+} in the crystal lattice introducing a cooperative Jahn–Teller tetragonal distortion. Consequently we have concentrated on a modelling study of insertion into Fe_3O_4.

3. Insertion Calculations

As noted earlier, Thackeray *et al.* (*1*) were unable to establish accurate structural information on lithiation of Fe_3O_4 from their X-ray intensity data owing to the low scattering power of X-rays by lithium. Nevertheless qualitative structural features were obtained from an analysis of the contributions from the ions to the structure factors of the observed reflections. The present work demonstrates how atomistic theoretical calculations can be used to examine lithiation of Fe_3O_4 and thus provide information of various insertion, aggregation, and diffusion processes.

In evaluating the influence of insertion on the transport properties of the material it is important to know the exact location of the inserted lithium. The location of the ions raises two questions. The first is related to the fact that the intercalate can occupy either the 8a or 16c site. The second concerns whether the insertion process proceeds with displacement of the 8a-Fe^{3+} ions into neighboring unoccupied 16c sites. As a method of answering these quesitons, the energies of formation on the various lattice locations are of interest. In this treatment, as in all previous defect studies, it is assumed that the lithium is fully ionized and enters the host lattice as an interstitial lithium. Since insertion reactions are generally controlled by the rate of solid-state diffusion (*13*) lithium transport properties through the 3D interstitial channels are also considered.

3.1 Methodology and Potentials

The atomistic simulations were performed using the CASCADE program (*14*) which employs the generalized Mott–Littleton procedure. The calculations are

TABLE I

SHORT-RANGE POTENTIALS AND SHELL-MODEL PARAMETERS USED FOR THE INSERTION STUDY

Interaction	A_o (eV)	A_t (eV)	ρ (Å)	C (eV Å^6)
Fe^{2+}. . . O^{2-}	694.1	599.4	0.3399	0.0
Fe^{3+}. . . O^{2-}	1102.4	976.6	0.3299	0.0
Li^{+}. . . O^{2-}	235.1	206.0	0.3544	0.0
O^{2-}. . . O^{2-}	22764.3	—	0.1490	27.88

Species	Y ($\|e\|$)	k (eV Å^{-2})
Fe^{2+}	2.00	10.92
Fe^{3+}	4.97	304.70
Li^{+}	1.00	10^5
O^{2-}	−2.207	27.29

Note. Cutoff = 1.50 lattice units.

based on the use of the Born model for the ionic solid and require specification of interatomic potentials representing the interaction both between host lattice ions and between host and defect species. It is necessary to include the effect of ionic polarizability which is represented by the shell model of Dick and Overhauser (*15*).

In the present study potential parameters for the host lattice, Fe_3O_4, are taken from the work of Lewis and Catlow (*16*). It is worth noting that these potentials have been successfully applied to the study of the defect structure and ion migration in Fe_3O_4 (*17*). Those for lithium were developed by empirical fitting to the lattice energy and crystal structure of Li_2O, which adopts the anti-fluorite structure. The short-range components of the Li. . .Li interaction were included, at least initially, but it was found that its effect on the final calculated energies was negligible. The shell-model and potential parameters used are presented in Table I. For a detailed discussion of the methodology and applications of our calculations we refer to Catlow and Mackrodt (*18*) and Catlow (*19*).

3.2 Results and Discussion

The energies of isolated lithium interstitials at both the tetrahedral (8a) and octahedral (16c) sites have been calculated to identify preferential insertion sites in the spinel framework and are reported in Table II. The relative magnitude of the formation energies on the two sites indicates that the 16c site is more favorable by ca. 1 eV—a result that is in accord with the experimental data and with the known properties of other spinel oxides.

TABLE II

FORMATION ENERGIES OF ISOLATED DEFECTS

Defect	E (eV)
$Li^{\cdot}$ (8a)	−0.91
$Li^{\cdot}$ (16c)	−1.88
Fe' (8a)	27.18
Fe' (16c)	28.15

As well as isolated defects, calculations were performed on clusters containing nearest-neighbor lithium interstitials on vacant octahedral sites. Binding energies with respect to component interstitials are reported to assist in the comparison of the different clusters. The results in Table III show that aggregation of the lithium, to yield small clusters of intercalates, may occur. This suggests that clusters could form as a precursor to the final ordered rock-salt structured phase. However, since

TABLE III

CLUSTERS OF LITHIUM ON OCTAHEDRAL (16c) SITES

Cluster	Binding energy (eV)
$2Li^{\cdot}$	−0.24
$3Li^{\cdot}$	−0.20
$4Li^{\cdot}$	1.35

Note. A negative value indicates the system is bound.

the cluster consisting of four lithium ions is unstable with a positive binding energy, it does not seem likely that this mode of aggregation would give rise to large defect clusters, although it is possible that other types of large aggregate could have higher stability.

Within the spinel structure each 8a tetrahedron shares all four faces with unoccupied 16c octahedra. It is thus possible to visualize that insertion of Li^+ ions into the 16c positions could lead to displacement of the 8a-Fe^{3+} into adjacent 16c sites, as a result of the close cation repulsion. Furthermore, the lithium is completely ionized in this material; the electron donated may be either fully delocalized or localized on the iron site (*20*). It has been argued that the electron is localized on the 8a-Fe^{3+} (*1*). Indeed, Chen *et al.* (*21*) have shown that the presence of reducible cations facilitates the uptake of Li^+ ions in spinels.

In Table IV the results of calculations of the change in lattice energy on inserting lithium and the subsequent creation of Fe^{2+} are presented. We have considered the cases in which the reduced iron atom is either on the 8a or the 16c site. Examination of the binding energies indicate that the clusters involving octahedral Fe^{2+} are more stable than the corresponding cluster of tetrahedral Fe^{2+}. Furthermore, the stabilization is greater for the simple pair cluster, $(Li \cdot Fe_o')$, and may predominate over all other simple aggregates. The presence of

TABLE IV

CLUSTERS OF Li^+ AND Fe^{2+}

Cluster	E (eV)	$B \cdot E^*$ (eV)
$(Li \cdot Fe_t')$	23.45	−1.85
$(Li \cdot Fe_o')$	23.40	−2.87
$(2Li \cdot 2Fe_t')$	46.61	−2.00
$(2Li \cdot 2Fe_o')$	47.31	−2.62

Note. t and o refer to the 8a and 16c sites, respectively.

* B · E = binding energy.

TABLE V

ENERGIES OF IONIZATION AND SUBLIMATION (*22*)

Term	E (eV)
I_{Li}	5.39
I_{Fe}	30.65
E_s	1.67

Note. I_{Li} = first ionization energy of Li; I_{Fe} = third ionization energy of Fe; E_s = sublimation energy of $Li_{(s)}$.

16c-Li^+, therefore, encourages 16c site occupancy of Fe^{2+}. This supports the models in which the insertion process proceeds with displacement of the tetrahedrally coordinated iron atom and in agreement with the proposed reaction pathway from X-ray and electrochemical data (*1*). It is seen in Table IV that the clusters in which Fe^{2+} occupies the 8a site are also bound. However, there is a ligand-field term which strongly favors the octahedral site for Fe^{2+}.

The principal contribution to the energy of insertion is the difference in chemical potential between electrons in the conduction band of the host and in lithium metal. By treating the electronic states as localized small polarons the energy of insertion can be given by:

$$E_I = (I_{Li} - I_{Fe}) + E_s + \Delta L,$$

where I_{Li} is the first ionization energy of lithium, I_{Fe} the third ionization energy of iron, E_s the sublimation energy of $Li_{(s)}$, and ΔL the lattice energy term associated with the $(Li \cdot Fe_o')$ pair. The latter term is calculated to be 23.40 eV and hence an insertion energy of −0.19 eV is obtained. Although there is no experimental value for comparison, our estimated energy, which is small and exothermic, seems a reasonable prediction (see Tables V and VI).

As commented already, insertion processes are dependent upon the rate of diffu-

TABLE VI

ENERGY OF INSERTION AND ENERGY OF ACTIVATION FOR LITHIUM ION MIGRATION

Term	E (eV)
E_I	−0.19
E_A	0.57

sion of the intercalate. Therefore, the examination of Li^+ ion mobility in Fe_3O_4 is of significant interest. For diffusion the important factor is the relative energy of the sites encountered by the Li^+ ion as it moves through the interstitial channels. The rate determining step and hence the activation energy is concerned with Li^+ ion hopping to adjacent interstitial sites.

For migration through the interconnected edge-shared octahedral (16c) sites we calculated an activation energy of 0.57 eV. There is at present no corresponding quantitative experimental data specifically for Fe_3O_4. There does, however, seem to be evidence for the activation energy for Li diffusion through framework-structured ternary oxides in the region of 0.5 eV (*20*), which would be consistent with the results of the calculations. The calculated activation energy suggests high lithium mobility even at room temperature through the vacant 16c sites of the close-packed array, which contains significant concentrations of iron on the 16d sites. The concentration of iron atoms is, therefore, not great enough to suppress percolation within the system. It is noted that no ordering process can take place without diffusion which is largely determined by the charge and size of ions in question. Since the Li^+ ion may diffuse quite easily, ordering in Fe_3O_4 containing lithium will occur.

It is also apparent that the diffusion rate of Li^+ ions in this close-packed structure is slower than those exhibited in layered structures. This fact is not unexpected when considering the rigid character of the spinel structure, which is volume-constrained, whereas layer structures are flexible in the c-direction.

4. Structural and Transport Properties of $LiFe_3O_4$

Lithiation of Fe_3O_4 results in the end composition corresponding to $LiFe_3O_4$ and involves a filling of the unoccupied 16c sites with Li^+ ions. The final product is a rock-salt-like structure with the following arrangement of the cations:

$$\{Li^+Fe^{2+}\}[Fe^{2+}Fe^{3+}]O_4,$$

where the braces and brackets enclose atoms in octahedral 16c and 16d sites, respectively. In order to accommodate the lithium the tetrahedrally coordinated iron has been displaced to octahedral (16c) sites, minimizing Li–Fe interactions. In this section we are concerned with the structural and ion migration properties of the rock-salt phase, paying particular attention to atomic ordering and lithium diffusion mechanisms.

4.1 Structural Modelling

Our first concern is with the construction of a satisfactory unit cell for $LiFe_3O_4$ and the subsequent lattice energy minimization. As outlined by Catlow (*19*) the minimum energy configuration is calculated from an initial structure. This approach is particularly useful when the initial structure consists of the ideal atomic positions. Hence the rock-salt arrangement is constructed from the ideal spinel unit cell but with lithium and iron occupying all the octahedral interstices. In Figs. 1 and 2 the structures of Fe_3O_4 and $LiFe_3O_4$ are illustrated schematically.

We note that the energy minimization includes the variation of the unit-cell vectors, i.e., under constant pressure conditions, as these parameters are not ac-

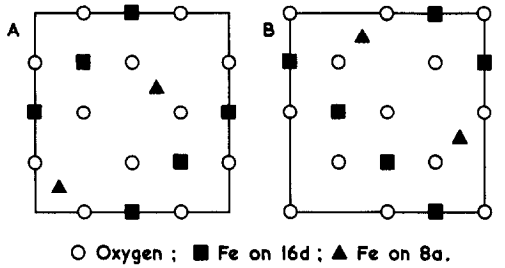

FIG. 1. The structure of Fe_3O_4 spinel in the (001) plane. (A) $z = 0$, ▲ at $z = \frac{1}{8}$; (B) $z = \frac{1}{4}$, ▲ at $z = \frac{3}{8}$.

curately known. The calculated lattice energies for $LiFe_3O_4$ and Fe_3O_4 are reported in Table VII. The difference in lattice energies, ΔE_L, is found to be 22.36 eV. On comparison with the formation energy of the (Li · Fe′) cluster, ΔE_L, is ca. 1 eV lower in energy than the value reported in Table IV. This confirms the energetic preference for the long-range ordering of the Fe^{2+} and Li^+ ions on the 16c sites and suggests that the rock-salt structure of the lithiated spinel is stabilized by insertion of up to one lithium per formula unit.

Examination of the 16d-Fe and oxygen positions in Fe_3O_4 reveals that the relative positions are virtually unchanged on lithiation to form $LiFe_3O_4$. This is in accord with diffraction data which show that the octahedral sublattice $[Fe_2]O_4$ remains intact during insertion and acts as a close-packed anion 3D framework (*1*). In Table VIII the

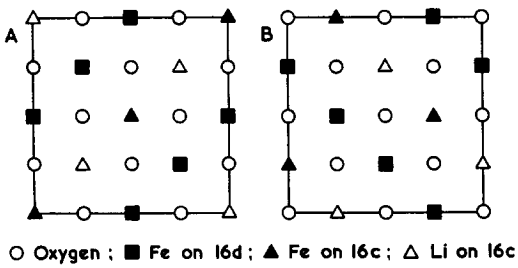

FIG. 2. The structure of the ordered rock-salt $LiFe_3O_4$ phase in the (001) plane. (A) $z = 0$; (B) $z = \frac{1}{4}$.

TABLE VII

CALCULATED LATTICE ENERGIES

Compound	E_L (eV)	ΔE_L (eV)
Fe_3O_4	−191.50	22.36
$LiFe_3O_4$	−169.14	

calculated lattice parameter for $LiFe_3O_4$ is compared with the experimental values for Fe_3O_4, $Li_{1.5}Fe_3O_4$, and FeO. We note that FeO is normally assigned to $Fm3m$ (a = 4.307 Å), but to allow direct comparison with the other structures it has been indexed to a super cell with $a = 2 \times 4.307$ Å. The calculations indicate that lithiation to $LiFe_3O_4$ results in an increase in the cubic lattice parameter from 8.396 to 8.450 Å, which represents a 1.93% volume expansion of the Fe_3O_4 unit cell, consistent with experiment.

4.2 Defect Structure and Lithium Diffusion

Our main concern in this section is the calculation of defect formation and activation energies for Li^+ ion diffusion in Li Fe_3O_4. Table IX presents the calculated energies for the formation of isolated vacancies and interstitials, which are combined to give the Frenkel and Schottky energies reported in Tables X and XI, respectively. One clear prediction follows from the results: the predominant mode of intrinsic disorder is of the lithium Frenkel type; lithium interstitial and vacancy disor-

TABLE VIII

LATTICE PARAMETERS

Compound	a_o (Å)
Fe_3O_4	8.396(exp)
FeO	8.614(exp)
$LiFe_3O_4$	8.450(calc)
$Li_{1.5}Fe_3O_4$	8.474(exp)

TABLE IX

ISOLATED DEFECT ENERGIES IN $LiFe_3O_4$

Defect	E (eV)
V'_{Li}	6.41
$Li_i^{\cdot}$	−4.82
V''_{Fe}	22.26
$Fe_i^{\cdot\cdot}$	−18.93
V'''_{Fe}	48.49
$Fe_i^{\cdot\cdot\cdot}$	−44.41
$V_O^{\cdot\cdot}$	23.22
O''_i	−13.78

TABLE XI

FORMATION ENERGIES OF SCHOTTKY DEFECTS

Defect	E (eV)	E (eV per defect)
Li_2O	6.27	2.09
FeO	5.89	2.94
Fe_2O_3	13.53	2.71
Fe_3O_4	20.64	2.95
$LiFe_3O_4$	23.16	2.90

der should therefore dominate in the pure material.

Since diffusion is controlled primarily by the energy parameters associated with the formation and migration of point defects, activation energies for Li^+ ion migration were also investigated. The mechanisms considered involve the Li^+ ion migrating by either (i) a vacancy jump, (ii) a direct interstitial jump, or (iii) an "interstitialcy" jump. These are illustrated in Fig. 3.

For the lithium vacancy jump the saddle-point has the migrating ion equidistant between the two lattice sites. Two mechanisms were considered for the direct interstitial migration involving edge-sharing and face-sharing tetrahedra. Finally the concerted or "interstitialcy" mechanism involves the correlated motion of ion pairs through face-sharing octahedra and tetrahedra.

Examination of the calculated activation energies, reported in Table XII, reveals that the lithium interstitial is the more mobile species via the interstitialcy mechanism, as opposed to the direct migration. A similar result was found for anion interstitial migration in UO_2 (*23*). Coexistence of

TABLE X

FORMATION ENERGIES OF FRENKEL DEFECTS

Defect	E (eV)	E (eV per defect)
Li^+	1.58	0.79
Fe^{2+}	3.34	1.67
Fe^{3+}	4.08	2.04
O^{2-}	9.44	4.72

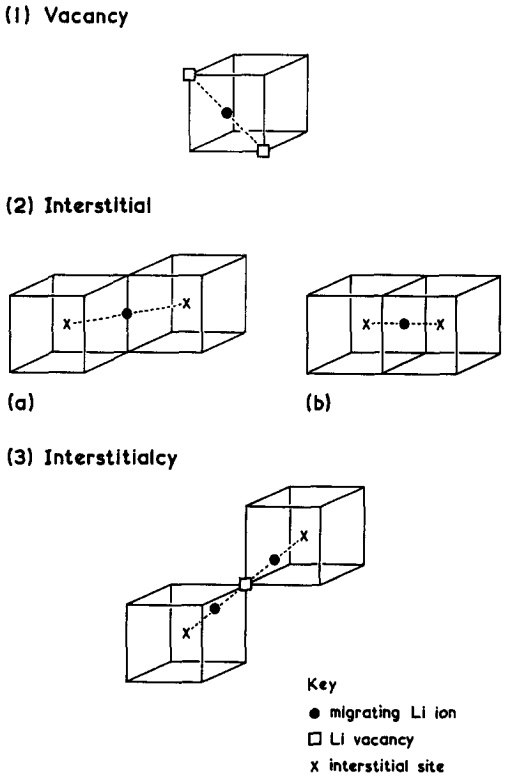

FIG. 3. Lithium diffusion mechanisms in the rock-salt structured $LiFe_3O_4$.

TABLE XII

ACTIVATION ENERGIES FOR LITHIUM ION MIGRATION IN $LiFe_3O_4$

Mechanism	E (eV)
Vacancy (collinear)	0.61
Vacancy (noncollinear)	2.24
Interstitial (face)	0.83
Interstitial (edge)	0.66
Interstitialcy	0.34

Li^+ ions on tetrahedral (8a) and octahedral (16c) positions thus provides continuous diffusion pathways through an interconnected 3D network of site faces rather than site edges.

Owing to the lack of experimental data on $LiFe_3O_4$ these calculations have a clear predictive value. However, the properties that emerge from the theoretical survey are broadly in line with models postulated from experiment (*1, 8*) and with those of other rock-salt structured materials.

5. Conclusions

Our discussion has drawn attention to four main features of lithium insertion into Fe_3O_4. First the lithium intercalate preferentially occupies the vacant octahedral (16c) site, and cluster pairs involving octahedral Fe^{2+} are more stable than the corresponding tetrahedral Fe^{2+} cluster. This supports the models in which insertion proceeds with reduction and displacement of the 8a-Fe^{3+}, in accord with the reaction pathway postulated from experiment. Second, we expect high Li^+ ion mobility although relatively slower than those exhibited in layer structured materials. Third, the investigation of $LiFe_3O_4$ confirms the long-range ordering of Fe^{2+} and Li^+ ions on the interconnected 16c array and suggests that the rock-salt structure of the lithiated Fe_3O_4 is stabilized by insertion of up to one lithium per formula unit. Finally, lithium Frenkel disorder emerges as the dominant mode of intrinsic defect in $LiFe_3O_4$ with the interstitialcy mechanism for Li^+ ion diffusion strongly favored.

The calculations described represent the first detailed application of atomistic simulation techniques to the study of lithium insertion. Since a wide range of oxides adopt the close-packed spinel structure, a great deal more future work remains in this field.

Acknowledgments

We are grateful to the SERC and to STC Components Ltd. for supporting this work.

References

1. M. M. THACKERAY, W. I. F. DAVID, AND J. B. GOODENOUGH, *Mater. Res. Bull.* **17,** 785 (1982).
2. J. B. GOODENOUGH, *in* "Solid Electrolytes" (P. Hagenmuller and W. van Gool, Eds.), Chap. 23, Academic Press, New York (1978).
3. J. B. GOODENOUGH, H. Y. P. HONG, AND J. A. KAFALAS, *Mater. Res. Bull.* **11,** 203 (1976).
4. M. S. WHITTINGHAM, *Science* **192,** 1126 (1976).
5. K. MIZUSHIMA, P. C. JONES, P. J. WISEMAN, AND J. B. GOODENOUGH, *Mater. Res. Bull.* **15,** 783 (1980).
6. M. S. WHITTINGHAM, *Prog. Solid State Chem.* **12,** 91 (1978).
7. J. B. GOODENOUGH, K. MIZUSHIMA, AND T. TAKEDA, *Japan. J. Appl. Phys.* **19,** 305 (1980).
8. L. A. DE PICCIOTTO AND M. M. THACKERAY, *Mater. Res. Bull.* **21,** 583 (1986).
9. D. G. WICKHAM AND W. J. CROFT, *J. Phys. Chem. Solids.* **7,** 351 (1958).
10. M. M. THACKERAY, W. I. F. DAVID, P. G. BRUCE, AND J. B. GOODENOUGH, *Mater. Res. Bull.* **18,** 461 (1983).
11. W. I. F. DAVID, M. M. THACKERAY, L. A. DE PICCIOTTO, AND J. B. GOODENOUGH, *J. Solid State Chem.* **67,** 316 (1987).
12. A. MOSBAH, A. VERBAERE, AND M. TOURNOUX, *Mater. Res. Bull.* **18,** 1375 (1983).
13. F. LÉVY, Ed., "Intercalated Layered Compounds," Reidel, Dordrecht (1979).
14. M. LESLIE, Daresbury Lab. Rep. DL/SCI/TM31T (1982).
15. B. G. DICK AND A. W. OVERHAUSER, *Phys. Rev.* **112,** 90 (1958).

16. G. V. LEWIS AND C. R. A. CATLOW, *J. Phys. C.* **18,** 1149 (1985).
17. G. V. LEWIS, C. R. A. CATLOW, AND A. N. CORMACK, *J. Phys. Chem. Solids* **46,** 1227 (1985).
18. C. R. A. CATLOW AND W. C. MACKRODT, Eds., "Computer Simulation of Solids," Lecture Notes in Physics, Vol. 166, Springer-Verlag, Berlin (1982).
19. C. R. A. CATLOW, *in* "Solid-State Chemistry: Techniques" (A. K. Cheetham and P. Day, Eds.), Chap. 7, Oxford Univ. Press (Clarendon), London/New York (1987).
20. I. D. RAISTRICK, *Solid State Ionics* **9** and **10,** 425 (1983).
21. C. J. CHEN, M. GREENBLATT, AND J. V. WASZCZAK, *Mater. Res. Bull.* **21,** 609 (1986).
22. W. E. DASENT, "Inorganic Energetics," Penguin, Baltimore (1970).
23. C. R. A. CATLOW, *Proc. R. Soc. London Ser. A* **353,** 533 (1977).